

Energy Dependence of State-to-State Reaction Probabilities for $\text{H}_2 + \text{OH} \rightarrow \text{H} + \text{H}_2\text{O}$ in Six Dimensions

Jiqiong Dai, Wei Zhu, and John Z. H. Zhang^{*,†}

Department of Chemistry, New York University, New York, New York 10003

Received: June 7, 1996[⊗]

We report benchmark time-dependent quantum calculation of state-to-state reaction probabilities for the title reaction in full dimensions (6D) using the widely used Schatz–Elgersma potential energy surface (PES). The time-dependent wave function is propagated using the diatom–diatom Jacobi coordinates and the energy-specific state-to-state reaction probabilities are obtained by using the correlation function method. All results reported here are for reaction resulting from the ground state of $\text{H}_2 + \text{OH}$ to various product states of $\text{H} + \text{H}_2\text{O}$ for total angular momentum $J = 0$. The present calculation shows that although the total reaction probability is a smooth function of energy, the final state-specific reaction probabilities show oscillatory structures as a function of collision energy for the title reaction.

I. Introduction

The time-dependent wave-packet approach has been shown for the past several years to be a powerful computational approach for large-scale quantum reactive scattering calculations. Benchmark quantum dynamics calculations for diatom–diatom reactions using the time-dependent wave-packet approach have been reported for several four-atom reaction systems in full-dimensional space^{1–7} and in planar geometry.^{8–10} So far the time-dependent methods have been applied primarily for calculating total reaction probabilities and cross sections for given initial states, i.e., summed over all product quantum states. The time-dependent wave-packet approach is particularly efficient for calculating final state-summed dynamics quantities because one does not need to propagate the wave packet into the product asymptotic region when final state resolution is not required. As shown in ref 2, the total reaction probability for a given initial state can be calculated as reactive flux at a dividing surface which is normally chosen to be near the transition-state region for optimal efficiency. In this flux approach, one simply uses an optical potential to absorb the wave function beyond the dividing surface and thus avoid entirely the calculation of numerous product asymptotic states.

However, in addition to total reaction probabilities and cross sections, one ultimately wants to study detailed product-state distribution which could provide much more detailed dynamics information for a chemical reaction. The complete state-to-state dynamics calculation is becoming more relevant in view of recent advances in the development of experimental techniques for state-specific detection of gas-phase chemical reactions. However, the state-to-state quantum dynamics calculation for four-atom reactions is a tremendously challenging task, both theoretically and computationally. The earliest quantum state-to-state attempt for $\text{H}_2 + \text{OH}$ reaction was made by reduced dimensionality calculations of Clary¹¹ and Wang and Bowman¹² in which only three coordinates are explicitly treated in dynamics calculations. The first full-dimensional state-to-state calculation has recently been reported for the reverse reaction $\text{H} + \text{H}_2\text{O}$ by Zhang and Light^{7,13} using the time-dependent wave-packet approach. In this letter we report some preliminary results of state-to-state reaction probabilities for the $\text{H}_2 + \text{OH}$ reaction in

full-dimensional space using the time-dependent wave-packet approach. The present state-to-state results are obtained by using a time-correlation function method to extract state-to-state **S** matrix elements for the $\text{H}_2 + \text{OH}$ reaction for total angular momentum $J = 0$ on the widely used Schatz–Elgersma potential energy surface (PES)^{14,15} slightly modified by Clary.¹¹ The methodology of the present calculation is briefly described in section II, and the results of calculations and discussions of the results are provided in section III.

II. Methodology

In this application, we use essentially the same method as for calculating total reaction probabilities for $\text{OH} + \text{H}_2$ in refs 1–3 to propagate the wave function. However, since we want to extract final state-specific reaction probabilities, we need to propagate the wave function all the way into the product asymptotic region that significantly complicates the calculation. The specific method we employed in this study to extract final state-specific dynamics information is based on the time-correlation function method proposed by Tannor and Weeks.¹⁶ In the present application, however, both the initial and final state wave packets are placed in the reactant and product asymptotic regions, respectively, as described in a previous paper.¹⁷

Using the time-correlation function method, the **S** matrix element is given by^{16,17}

$$S_{fi}(E) = \frac{1}{2\pi\hbar a_{\alpha i}(E) a_{\beta f}^*(E)} \int_{-\infty}^{\infty} dt e^{(i\hbar)Et} \langle \chi_{\beta f}^- | e^{-(i\hbar)Ht} | \chi_{\alpha i}^+ \rangle$$

$$= \frac{1}{2\pi\hbar a_{\alpha i}(E) a_{\beta f}^*(E)} \int_{-\infty}^{\infty} dt e^{(i\hbar)Et} C_{fi}(t) \quad (1)$$

where χ^\pm is the initial (+) and final (−) wave packet for a given initial and final state, respectively, and $C_{fi}(t)$ is the correlation function defined as $C_{fi}(t) = \langle \chi_{\beta f}^- | e^{-(i\hbar)Ht} | \chi_{\alpha i}^+ \rangle$. A detailed explanation of various quantities in eq 1 can be found in ref 17. Since the total number of open channels in the product side ($\text{H} + \text{H}_2\text{O}$) is very large, about 1000 channels (energetically accessible rovibrational states of H_2O), the calculation to obtain complete final-state distribution of H_2O is tedious in the time correlation function approach. In the present application, we calculate all the time-correlation functions $C_{fi}(t)$ at each time step for all the final states *f* and store them on computer disk.

[†] Alfred P. Sloan Fellow and Camille Dreyfus Teacher–Scholar.

[⊗] Abstract published in *Advance ACS Abstracts*, August 1, 1996.

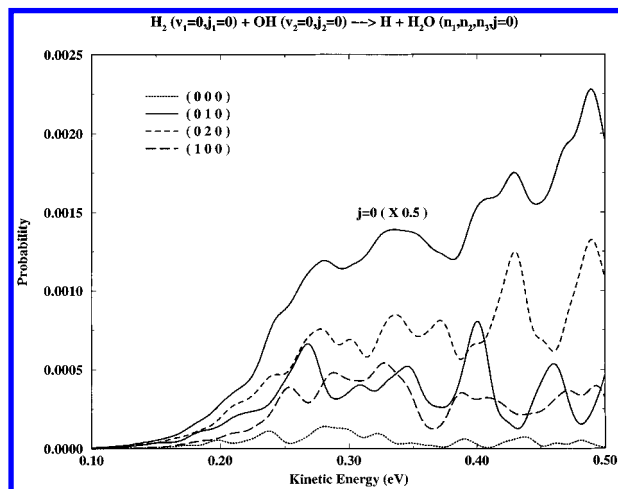


Figure 1. Energy dependence of product vibrational state-specific reaction probabilities from the reaction $\text{OH}(00) + \text{H}_2(00) \rightarrow \text{H}_2\text{O}(v,j=0)$ for zero total angular momentum of H_2OH . The vibrational state label of H_2O (v_1, v_2, v_3) follows the standard convention. The highest curve is the vibrationally summed reaction probability for $j = 0$ but reduced by a factor of two before being plotted. Only the first four open vibrational states are explicitly shown in Figure 1.

These time-correlation functions are later retrieved to generate individual **S** matrix element for any desired energy by a simple Fourier transform according to eq 1. This seems to be a main attractive feature of the time-correlation function method because one can essentially obtain individual **S** matrix elements within a continuous spectrum of scattering energy.

III. Results and Discussions

The present calculation employed more than 4026 coupled angular momentum basis functions and a numerical grid extending to 12 atomic units (au) in the H_2 diatomic coordinate and 12 au in the OH to H_2 radial coordinate. Detailed numerical aspects of the calculation are not given here but will be provided in a detailed paper later. The results presented in this letter are for zero total angular momentum of the H_2OH system and for reactant $\text{H}_2 + \text{OH}$ at ground rovibrational state. In the following, we use j to denote the angular momentum quantum number of the triatomic product H_2O . The time step used in the wave-packet propagation by the split-operator method is 10 au, which is sufficient in the present study. A total propagation time of 10 000 au is used to complete the wave-packet propagation. As mentioned in the previous section, once the time-correlation function is calculated and stored in computer disk, we can obtain individual **S** matrix elements for any desired energies of interest within the range of initial and final wave packets. In fact, we calculated **S** matrix elements for all the product states at more than 1000 scattering energies.

Figure 1 is a plot of final vibrational state-specific reaction probabilities (**S** matrix squared) of H_2O at $j = 0$ rotation as a function of kinetic energy. First we observe that the individual state-to-state reaction probability is generally very small (on the order of 10^{-5} for the ground vibrational state and to about 10^{-3} for higher vibrational states). Second, the individual reaction probabilities are generally oscillatory as a function of collision energy. In Figure 1, we only plotted first four vibrational states out of more than two dozen open vibrational states. The spectroscopic assignment of H_2O vibrational states on the Schatz–Elgersma potential energy surface is difficult because the H_2O potential deviates substantially from the experimental results and most vibrational states are mixed. For $j = 0$ rotation of H_2O , we assigned the first four states using the standard notation for triatomic vibrations as shown in Figure

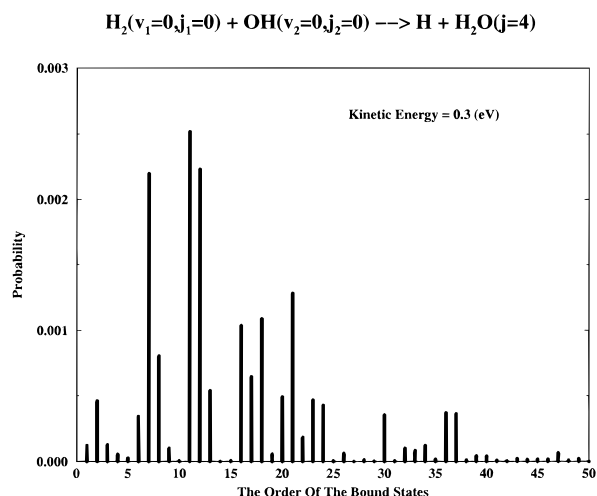


Figure 2. Product vibrational state distribution of H_2O from the reaction $\text{H}_2(00) + \text{OH}(00) \rightarrow \text{H} + \text{H}_2\text{O}(v,j=5)$ for zero total angular momentum of H_2OH at a kinetic energy of 0.3 eV.

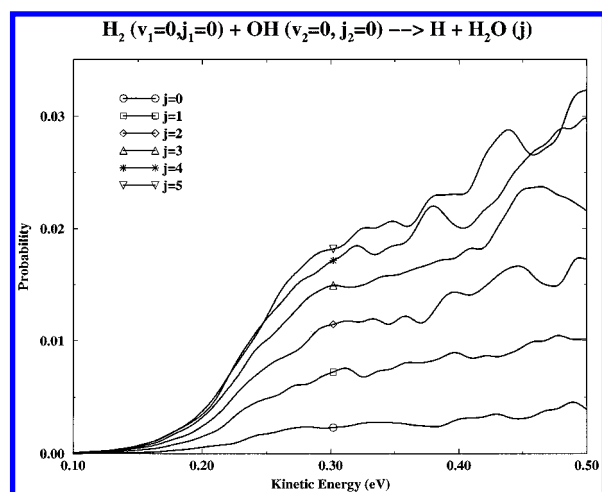


Figure 3. Energy dependence of product rotation-specific (vibrationally summed) reaction probabilities from the reaction $\text{OH}(00) + \text{H}_2(00) \rightarrow \text{H}_2\text{O}(\text{all } v,j)$ where j ranges from 0 to 5.

1. We note that the $\text{OH} + \text{H}_2$ reaction in the ground state favors vibrationally excited H_2O product, in particular bending excited H_2O product on the Schatz–Elgersma PES. The highest curve shown in Figure 1 is the vibration-summed reaction probability (summed over all open vibrational states) for H_2O at $j = 0$. Here we see that even partially summed probability shows oscillatory structure as a function of collision energy.

We show in Figure 2 the vibrational state distribution of H_2O at $j = 4$ rotation for a fixed collision energy of 0.3 eV. The vibrational states, however, are not yet assigned because of difficulties mentioned above. In addition, the proliferation of open channels with the increase of rotational quantum number j of H_2O makes the task of assignment even more difficult for high- j states. We therefore postpone this task to a future study. We should mention here that these individual state-to-state reaction probabilities are quite difficult to converge to high accuracy, and we believe they might be substantial errors associated with some individual state-to-state probabilities despite our best effort to converge them. However, the overall picture of the energy dependence of these probabilities as shown in Figure 1 should not be seriously affected.

The partially summed probabilities are better converged than the individual state-to-state ones. In Figures 3 and 4 we show rotation-specific but vibration-summed reaction probabilities plotted as functions of collision energy. We can see that for

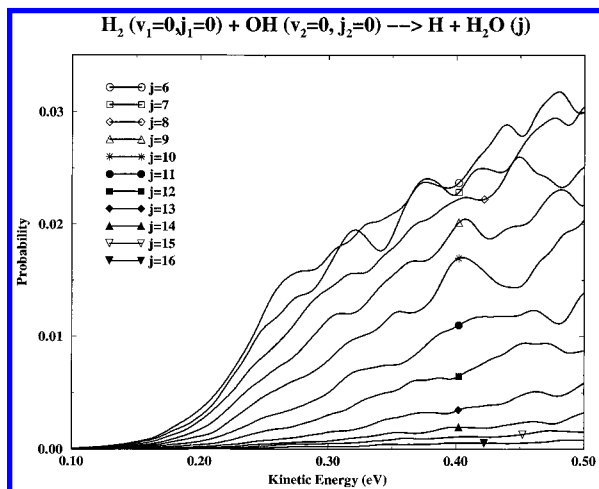


Figure 4. Similar to Figure 3 but for j in the range 6–16.

most energies, the rotation state distribution peaks around $j = 5-7$. Also these partially summed probabilities are not as oscillatory as individual state-to-state ones in Figure 1. As is shown in an earlier study,² the energy dependence of the total reaction probability (summed over all rovibrational states) is completely smooth. Most recently, a similar state-to-state calculation of reaction probabilities for the title reaction but using flux method to extract product-state distribution of reaction probability is also being completed.¹⁸ The transition probabilities from the ground-state reagent to ground-state product from refs 13 and 18 and the present calculation are within 10% of each other. Other state-to-state reaction probabilities agree with those of ref 18 within the convergence limit of each calculation (average about 30% for individual state-to-state and 10% for partially summed probabilities).

To summarize, the main advantage of the time-correlation function approach is that one can obtain selected S matrix element or probability for any desired energies without additional computational effort. However, it is a challenge if one wants to obtain the complete product-state distribution when

the number of open product channels is very large such as in the present case. The availability of rigorous quantum mechanical calculation of state-to-state S matrix element or reaction probability for four-atom reactions such as reported in this letter will make it possible for comparing quantum results with state-to-state experimental results for some four-atom reactions in the near future. It will also serve to provide a more stringent test for various approximate quantum methods such as reduced dimensionality method in 3D^{11,12} and 4D⁸⁻¹⁰ and mixed quantum/classical method.¹⁹

Acknowledgment. This work is supported by the Division of Chemical Sciences, Office of Basic Energy Sciences, Office of Energy Research, U.S. Department of Energy, under Grant No. DE-FG02-94ER14453.

References and Notes

- (1) Zhang, D. H.; Zhang, J. Z. H. *J. Chem. Phys.* **1993**, *99*, 5615; **1994**, *100*, 2697.
- (2) Zhang, D. H.; Zhang, J. Z. H. *J. Chem. Phys.* **1994**, *101*, 5615.
- (3) (a) Zhang, D. H.; Zhang, J. Z. H. *Chem. Phys. Lett.* **1995**, *232*, 370. (b) Zhang, D. H.; John, J. Z. H.; Zhang, Y.; Wang, D.; Zhang, Q. *J. Chem. Phys.* **1995**, *102*, 7400.
- (4) Zhang, Y.; Zhang, D.; Li, W.; Zhang, Q.; Wang, D.; Zhang, D. H. *J. Phys. Chem.* **1995**, *99*, 16824.
- (5) Zhang, D. H.; Zhang, J. Z. H. *J. Chem. Phys.* **1995**, *103*, 6512.
- (6) Neuhauser, D. *J. Chem. Phys.* **1994**, *100*, 9272.
- (7) Zhang, D. H.; Light, J. C. *J. Chem. Phys.* **1996**, *104*, 4544.
- (8) Echave, J.; Clary, D. C. *J. Chem. Phys.* **1994**, *100*, 402.
- (9) Thompson, W. H.; Miller, W. H. *J. Chem. Phys.* **1994**, *101*, 8620.
- (10) Goldfield, E. M.; Gray, S. K.; Schatz, G. C. *J. Chem. Phys.* **1995**, *102*, 8807.
- (11) Clary, D. C. *J. Chem. Phys.* **1991**, *95*, 7298.
- (12) Wang, D.; Bowman, J. M. *J. Chem. Phys.* **1992**, *96*, 8906.
- (13) Zhang, D. H.; Light, J. C. *J. Chem. Phys.*, in press.
- (14) Walch, S. P.; Dunning Jr., T. H. *J. Chem. Phys.* **1980**, *72*, 1303.
- (15) Schatz, G. C.; Elgersma, H. *Chem. Phys. Lett.* **1980**, *73*, 21.
- (16) Tannor, D. J.; Weeks, D. E. *J. Chem. Phys.* **1993**, *98*, 3884.
- (17) Dai, J.; Zhang, J. Z. H. *J. Phys. Chem.* **1996**, *100*, 6898.
- (18) Zhu, W.; Dai, J.; Zhang, J. Z. H.; Zhang, D. H., submitted to *J. Chem. Phys.*
- (19) Balakrishnan, N.; Billing, G. D. *J. Chem. Phys.* **1994**, *101*, 2785.

JP961690P